Scalable Optimization Methods for Distribution Networks With High PV Integration

Swaroop S. Guggilam, *Student Member, IEEE*, Emiliano Dall'Anese, *Member, IEEE*, Yu Christine Chen, *Member, IEEE*, Sairaj V. Dhople, *Member, IEEE*, and Georgios B. Giannakis, *Fellow, IEEE*

***Abstract*—This paper proposes a suite of algorithms to determine the active- and reactive-power setpoints for photovoltaic (PV) inverters in distribution networks. The objective is to optimize the operation of the distribution feeder according to a variety of performance objectives and ensure voltage regulation. In general, these algorithms take a form of the widely studied ac optimal power flow (OPF) problem. For the envisioned application domain, nonlinear power-flow constraints render pertinent OPF problems nonconvex and computationally intensive for large systems. To address these concerns, we formulate a quadratic constrained quadratic program (QCQP) by leveraging a linear approximation of the algebraic power-flow equations. Furthermore, simplification from QCQP to a linearly constrained quadratic program is provided under certain conditions. The merits of the proposed approach are demonstrated with simulation results that utilize realistic PV-generation and load-profile data for illustrative distribution-system test feeders.**

***Index Terms*—Distribution networks, linearization, optimization, PV systems.**

I. Introduction

THE methods proposed in this paper seek contributions in the domain of next-generation distribution-system operations and control by leveraging scalable convex optimization approaches. The increased penetration of PV systems has highlighted pressing needs to address power quality and reliability concerns. Therefore, systematic means to operate distribution networks with high PV penetration will be key to ensure a sustainable capacity growth with limited need for transmission expansion.

Recent efforts in the domain of PV integration are focused on inverters deviating away from nominal maximum power outputs to provide reactive power support and curtail active power as required. For instance, local active power control strategies proposed in [1] and [2] are grounded on the premise of curtailing active power from inverters based on the observed nodal voltages. Similarly, low power factors and possibly high network currents—which may lead to conductor overheating and power losses—can occur if local reactive-power control strategies are used [3]–[5]. Focusing on network-wide optimality, an OPF-based Optimal Inverter Dispatch (OID) strategy was proposed in [6], where the SDP relaxation for AC power flow equations (see, e.g., [7]) was leveraged to obtain a strategy to dispatch network-wide-optimal setpoints for PV inverters. However, for a balanced network with N nodes, this problem requires $\mathcal{O}(N^2)$ optimization variables; consequently, this approach may become computationally expensive as the distribution-system size grows [8], even when parallel decomposition arguments for SDP programs are advocated [9]. A notable reference in this regard is the recently proposed sparsity-exploiting SDP formulation in [10] in which number of variables do not scale as $\mathcal{O}(N^2)$. Another pertinent reference is a Second Order Cone (SOC) relaxation of the OPF problem proposed in [11]. Using the SOC relaxation, a rendition of the OPF problem for networks with approximately 3000 buses has been solved in around 30 seconds [12]. We adopt an alternate perspective to tackle scalability in this work. In contrast to the relaxations advocated in the references above, we focus on obtaining linear relationships between network voltages and nodal power injections, which bypasses non-convexity in OPF problems and yields a convex problem formulation. In particular, we propose a Scalable Optimal Inverter Dispatch algorithm (SOID) using a recently proposed linear approximation to the power flow equations [13], [14]. This problem formulation address a different suite of Optimal Power Flow problems, wherein, along with voltage we also find active- and reactive-power setpoints for PV inverters. The proposed schemes required only $\mathcal{O}(N)$ optimization variables, and leads to a convex Linearly Constrained Quadratic Program (LCQP). Furthermore, when the cost is linear and real-power (or reactive-power) compensation alone is implemented, the SOID is in fact a linear program.

Manuscript received September 18, 2015; revised January 15, 2016 and March 7, 2016; accepted March 8, 2016. Date of publication April 4, 2016; date of current version June 17, 2016. The work of S. S. Guggilam, S. V. Dhople, and G. B. Giannakis were supported in part by the National Science Foundation under Grant CCF 1423316, Grant CyberSEES 1442686, and Grant CAREER Award ECCS-1453921, and in part by the Institute of Renewable Energy and the Environment, University of Minnesota, under Grant RL-0010-13. The work of E. Dall'Anese was supported by the Laboratory Directed Research and Development Program at the National Renewable Energy Laboratory. Paper no. TSG-01151-2015.

S. S. Guggilam, S. V. Dhople, and G. B. Giannakis are with the Department of Electrical and Computer Engineering, and the Digital Technology Center, University of Minnesota, Minneapolis, MN 55455 USA (e-mail: guggi022@umn.edu; sdhople@umn.edu; georgios@umn.edu).

E. Dall'Anese is with the National Renewable Energy Laboratory, Golden, CO 80401 USA (e-mail: emiliano.dallanese@nrel.gov).

Y. C. Chen is with the Department of Electrical and Computer Engineering, University of British Columbia, Vancouver, BC V6T 1Z4, Canada (e-mail: chen@ece.ubc.ca).

Color versions of one or more of the figures in this paper are available online at http://ieeexplore.ieee.org.

Digital Object Identifier 10.1109/TSG.2016.2543264

The key insight that this paper leverages to develop the optimization problems is a linear approximation of the nonlinear power flow expressions in rectangular coordinates [13], [14]. A variety of methods exploiting linearizations of the nonlinear power flow equations have been proposed in the literature. For instance, linear non iterative power flow algorithms considering only active power flows are proposed in [15] and [16]. Relaxed AC OPF problems obtained by linearizing just the power flow balance equations have been proposed in [17]–[20]. Different from the approaches above, we leverage a closed-form linear approximation for the voltages across the network [13], [14] to formulate computationally tractable optimization problems.

Compared to semidefinite programming (SDP) methods in our original work [6], simulations for a modified IEEE 123-node system demonstrate substantial computational speed improvements. Furthermore, we remark that while we consider single-phase settings, the linear approximations for the solutions to the power flow problem can be extended to cover multi-phase setups, following which, adopting approaches akin to the ones in [15], [17], and [21], the methods proposed here can be tailored to multi-phase setups. While these optimization problems for multi-phase settings are beyond the scope of this manuscript, they present compelling options for future work.

To further promote customer privacy while guaranteeing scalability of the algorithms with limited information exchanges, we also propose a distributed version of the problem setup leveraging the alternating direction method of multipliers (ADMM) [22]–[24]. Convergence is faster if ADMM is implemented in comparison to other distributed solution approaches such as the sub-gradient method [25], [26]. The SOID problem discussed above can be decomposed as a sum of utility optimization and customer based optimization objectives. Utility optimization includes network performance objectives like power losses, whereas customer based optimization includes maximizing their monetary objectives (e.g., minimizing the amount of active power to be curtailed). A two-way exchange of information is required to implement the above setup. Once the optimal setpoints are computed, they are dispatched to inverters, where we assume that local regulation capability implements the desired output real and reactive power.

To summarize, the contributions of this paper are as follows. First, we leverage a linearized version of the power flow equations in rectangular coordinates tailored to distribution networks to formulate an OPF-type problem with direct applications to distribution networks with PV systems. The formulated SOID problem (and accompanying special case tailored for resistive-dominant networks) can be formulated to meet performance objectives of minimizing power losses and voltage deviations from the nominal. Finally, to further promote scalability, we propose a distributed version of the problem that can be solved with ADMM.

The remainder of this paper is organized as follows. In Section II, the mathematical notation and network model used throughout the paper are described, and an approximate expression for the voltages is derived from linearization of the power-flow equations expressed in rectangular coordinates. Section III presents the SOID problem formulation along with the distributed implementation leveraging ADMM. In Section IV, we provide various case studies and simulation results to demonstrate the applicability of the method, and demonstrate computational savings compared to our previous efforts that leveraged SDP relaxations of the OPF problem. Finally, concluding remarks and some directions for future work are highlighted in Section V.

II. Preliminaries and Power System Model

In this section, we first establish notation and then describe the power-system model that is utilized in the remainder of the manuscript. We also develop the linearized model that relates the voltages in the network to power injections.

A. Notation

The matrix inverse is denoted by $(\cdot)^{-1}$, transpose by $(\cdot)^{\mathrm{T}}$, complex conjugate by $(\cdot)^*$, real and imaginary parts of a complex number by $\mathrm{Re}\{\cdot\}$ and $\mathrm{Im}\{\cdot\}$, respectively, magnitude and phase of a complex scalar by $|\cdot|$ and $\angle(\cdot)$, respectively and $\mathrm{j} \coloneqq \sqrt{-1}$. A diagonal matrix formed with diagonal entries composed of entries of vector x is denoted by $\mathrm{diag}(x)$. A diagonal matrix formed with the lth entry given by x_l/y_l is denoted by $\mathrm{diag}(x/y)$, where x_l and y_l are the lth entries of the vectors x and y, respectively and a diagonal matrix with the lth entry given by x_l^{-1} is denoted as $\mathrm{diag}(1/x)$. For a matrix X, X_{mn} returns the entry in the m row and n column of X. The $N \times 1$ vectors with all ones and all zeros are denoted by 1_N and 0_N, respectively. The spaces of $N \times 1$ real-valued and complex-valued vectors are denoted by $\mathbb{R}^N$ and $\mathbb{C}^N$, respectively; $\mathbb{T}^N$ denotes the N-dimensional torus.

B. Network Model

Consider a single-phase distribution network with $N+1$ nodes collected in the set $\mathcal{N}$ and distribution lines collected in the set $\mathcal{E}$. Define the set $\mathcal{N}' \subset \mathcal{N}$ to include all nodes except the $N+1$ node, i.e., $\mathcal{N}' = \mathcal{N} \backslash \{N+1\}$. At H of these $N+1$ nodes (collected in the set $\mathcal{H}$), we assume PV systems are installed with inverters capable of responding to real- and reactive-power dispatch commands. The $N+1$ node models the secondary of the step-down distribution transformer, and is assumed to be the slack bus. Lines are represented by the set of edges $\mathcal{E} \coloneqq \{(m,n)\} \subset \mathcal{N} \times \mathcal{N}$. Finally, note that $(\cdot)_{(m,n)}$ represents an electrical variable corresponding to the (m,n) line.

Let $I = [I_1, \ldots, I_N]^{\mathrm{T}}$, $V = [V_1, \ldots, V_N]^{\mathrm{T}} \in \mathbb{C}^N$ and $S = [S_1, \ldots, S_N]^{\mathrm{T}}$ where $I_\ell \in \mathbb{C}$ denotes the current injected into bus ℓ, $V_\ell = |V|_\ell \angle \theta_\ell \in \mathbb{C}$ represents the voltage phasor at bus ℓ and $S_\ell = P_\ell + \mathrm{j}Q_\ell$ denotes the complex-power bus injected at bus ℓ. In rectangular coordinates, we have $V = V_{\mathrm{re}} + \mathrm{j}V_{\mathrm{im}}$, where $V_{\mathrm{re}}, V_{\mathrm{im}} \in \mathbb{R}^N$ denote the real and imaginary components of V. Further, we will define $|V| = [|V|_1, \ldots, |V|_N]^{\mathrm{T}} \in \mathbb{R}^N_{>0}$ and $\theta = [\theta_1, \ldots, \theta_N]^{\mathrm{T}} \in \mathbb{T}^N$, which we will use subsequently. The available active power at nodes with PV systems (based on the incident irradiance) is denoted by the vector $P_{\mathrm{av}} \in \mathbb{R}^N_{\geq 0}$. The active powers curtailed

by the inverters are collected in $P_c \in \mathbb{R}^N_{\geq 0}$; and $Q_c \in \mathrm{R}^N$ collects the reactive powers generated/consumed by the PV inverters. Active- and reactive-power loads are collected in $P_d \in \mathbb{R}^N$ and $Q_d \in \mathbb{R}^N$ respectively. (Entries of P_{av}, P_c, and Q_c are zero if there are no PV systems at the corresponding node.)

The electrical network operation in sinusoidal steady state is described by Kirchhoff's current law as follows:

$$\begin{bmatrix} I \\ I_{N+1} \end{bmatrix} = \begin{bmatrix} Y & \overline{Y} \\ \overline{Y}^{\mathrm{T}} & \tilde{y} \end{bmatrix} \begin{bmatrix} V \\ V_\circ e^{j\theta_\circ} \end{bmatrix} \tag{1}$$

where $V_\circ e^{j\theta_\circ}$ is the slack-bus voltage with $V_\circ$ denoting the voltage magnitude at the secondary of the step-down transformer feeding the network. Hereafter, without loss of generality, we will consider $V_\circ = 1$ and $\theta_\circ = 0$ for our discussion. Dimensions of the entries of the admittance matrix are as follows: $\overline{Y} \in \mathbb{C}^N$, $Y \in \mathbb{C}^{N\times N}$, and $\tilde{y} \in \mathbb{C}\backslash\{0\}$. Also, we will find it useful to decompose $Y = G + jB$, where G and $B \in \mathbb{R}^{N\times N}$ are conductance and susceptance matrices respectively. Current injected into slack bus is given by I_{N+1}. The vector of shunt admittances can be extracted as

$$Y1_N + \overline{Y} = Y_{sh} = G_{sh} + jB_{sh} \tag{2}$$

where $Y_{sh} \in \mathbb{C}^N$, G_{sh} and $B_{sh} \in \mathbb{R}^N$.

C. Approximate Expression for the Voltages

We begin with complex-power balance, which can be written with the aid of (1) as follows:

$$S = \mathrm{diag}(V)I^* = \mathrm{diag}(V)\left(Y^*V^* + \overline{Y}^*\right). \tag{3}$$

Recall that we denote: $P_{av} \in \mathbb{R}^N$ as the available power (based on the incident irradiance), $P_c \in \mathbb{R}^N$ as the active power curtailed, $P_d \in \mathbb{R}^N$ as the active-power load, and note that similar definitions follow for reactive-power related variables. Note that entries of P_{av} and P_c are non-zero only if the corresponding node is connected to a PV system. With these definitions in mind, it follows that:

$$S = (P_{av} - P_c - P_d) + j(Q_c - Q_d). \tag{4}$$

Let the actual solution to (3) be denoted by $V \in \mathbb{C}^N$. We linearize (3) by expressing $V = V_{nom} + \Delta V$, where $V_{nom} = |V_{nom}|\angle\theta_{nom} \in \mathbb{C}^N$ is some pre-defined nominal voltage vector, and ΔV captures perturbations around V_{nom}. Consider the following choice of nominal voltage, which also corresponds to the voltage across the network with zero current injections:

$$V_{nom} = -Y^{-1}\overline{Y}. \tag{5}$$

With this choice of nominal voltage, it is easy to show that by neglecting higher-order terms in (3), we get the following solution for ΔV (details are in [14]):

$$\Delta V = Y^{-1}\mathrm{diag}\left(1/V^*_{nom}\right)S^*. \tag{6}$$

Then, expanding the terms in (6) and considering the real and imaginary components of ΔV provides the following equations:

$$\Delta V_{re} = \left(R\ \mathrm{diag}\left(\frac{\cos\theta_{nom}}{|V_{nom}|}\right) - X\ \mathrm{diag}\left(\frac{\sin\theta_{nom}}{|V_{nom}|}\right)\right)P + \left(X\ \mathrm{diag}\left(\frac{\cos\theta_{nom}}{|V_{nom}|}\right) + R\ \mathrm{diag}\left(\frac{\sin\theta_{nom}}{|V_{nom}|}\right)\right)Q, \tag{7}$$

$$\Delta V_{im} = \left(X\ \mathrm{diag}\left(\frac{\cos\theta_{nom}}{|V_{nom}|}\right) + R\ \mathrm{diag}\left(\frac{\sin\theta_{nom}}{|V_{nom}|}\right)\right)P - \left(R\ \mathrm{diag}\left(\frac{\cos\theta_{nom}}{|V_{nom}|}\right) - X\ \mathrm{diag}\left(\frac{\sin\theta_{nom}}{|V_{nom}|}\right)\right)Q, \tag{8}$$

where $P = P_{av} - P_c - P_d$ and $Q = Q_c - Q_d$ and $Y^{-1} = R + jX$.

Notice that $|V| = |V_{nom}| + \Delta V_{re}$ and $\theta = \theta_{nom} + \Delta V_{im}$ serve as first-order approximations to the voltage magnitudes and phases across the distribution network, respectively, when $\theta_{nom} \approx 0_N$. In the present setting, this is true when shunt impedances are negligible, i.e., $Y_{sh} = 0_N$. Furthermore, from (2) and (5), we see that $Y1_N + \overline{Y} = 0_N$, and $|V_{nom}| = 1_N$; as a result of which (7) and (8) simplify as below:

$$\Delta V_{re} = R\ P + X\ Q, \quad \Delta V_{im} = X\ P - R\ Q. \tag{9}$$

Finally, with the above discussions and approximations in place, we recognize that the voltage magnitude at the n-th bus is approximately given by

$$|V|_n \approx 1 + \sum_{\ell\in\mathcal{N}'} R_{n\ell}P_\ell + X_{n\ell}Q_\ell, \quad \forall\, n \in \mathcal{N}'. \tag{10}$$

III. Optimization Problem Formulation

In this section we begin by formulating different components of the cost function for the optimization problem. Next, we will describe the general SOID problem, consider a special case, and also present a distributed solution approach to the problem that promotes scalability.

A. Cost Function

The formulation of the cost function encapsulates a variety of power-quality and customer-oriented objectives. In particular, we will consider the weighted sum of the following functions to compose the optimization-problem cost function:

$$\rho(V) = \sum_{(m,n)\in\mathcal{E}} \mathrm{Re}\left\{y^*_{mn}\right\}\Big((\mathrm{Re}\{V_m\} + \mathrm{Re}\{V_n\})^2 + (\mathrm{Im}\{V_m\} + \mathrm{Im}\{V_n\})^2\Big), \tag{11}$$

$$\phi(P_c, Q_c) = \sum_{h\in\mathcal{H}} a_h P^2_{c,h} + b_h P_{c,h} + c_h Q^2_{c,h} + d_h|Q_{c,h}|, \tag{12}$$

$$\nu(V) = \sum_{n\in\mathcal{N}}\left(|V|_n - \frac{1}{N+1}\sum_{\ell\in\mathcal{N}}|V|_\ell\right)^2. \tag{13}$$

Above, function ρ denotes the real-power losses in the network; the function ϕ establishes a quadratic cost on the curtailed active power and generated/consumed reactive

power, and finally, the function ν attempts to minimize voltage deviations from the average. The choice of constants a_h, b_h, c_h, and d_h in (12) can be based on agreements between customer and utility. Note that the derivation for the expression corresponding to the losses (11) is provided in the Appendix.

B. SOID Problem: General Case

Using the functions defined in (11)-(13), let the overall cost function to be optimized be denoted by C_{opt}, and defined as follows:

$$C_{\text{opt}}(V, P_{\text{c}}, Q_{\text{c}}) = c_\rho \rho(V) + c_\phi \phi(P_{\text{c}}, Q_{\text{c}}) + c_\nu \nu(|V|), \quad (14)$$

where c_ρ, c_ϕ, and c_ν are weighting constants. Subsequently, the SOID problem is formulated as follows:

$$\begin{aligned}
\min_{V, P_{\text{c}}, Q_{\text{c}}} \quad & C_{\text{opt}}(V, P_{\text{c}}, Q_{\text{c}}) && (15a)\\
\text{subject to} \quad & \text{Re}\{V_n\} = 1 + \sum_{\ell \in \mathcal{N}'} \big(R_{n\ell}\big(P_{\text{av},\ell} - P_{\text{c},\ell} - P_{\text{d},\ell}\big) \\
& \qquad + X_{n\ell}\big(Q_{\text{c},\ell} - Q_{\text{d},\ell}\big)\big), \forall\, n \in \mathcal{N}' && (15b)\\
& \text{Im}\{V_n\} = \sum_{\ell \in \mathcal{N}'} \big(X_{n\ell}\big(P_{\text{av},\ell} - P_{\text{c},\ell} - P_{\text{d},\ell}\big) \\
& \qquad - R_{n\ell}\big(Q_{\text{c},\ell} - Q_{\text{d},\ell}\big)\big), \forall\, n \in \mathcal{N}' && (15c)\\
& V_{\min} \le 1 + \sum_{\ell \in \mathcal{N}'} R_{n\ell}\big(P_{\text{av},\ell} - P_{\text{c},\ell} - P_{\text{d},\ell}\big) \\
& \qquad + \sum_{\ell \in \mathcal{N}'} X_{n\ell}\big(Q_{\text{c},\ell} - Q_{\text{d},\ell}\big) \forall\, n \in \mathcal{N}' && (15d)\\
& V_{\max} \ge 1 + \sum_{\ell \in \mathcal{N}'} R_{n\ell}\big(P_{\text{av},\ell} - P_{\text{c},\ell} - P_{\text{d},\ell}\big) \\
& \qquad + \sum_{\ell \in \mathcal{N}'} X_{n\ell}\big(Q_{\text{c},\ell} - Q_{\text{d},\ell}\big) \forall\, n \in \mathcal{N}' && (15e)\\
& 0 \le P_{\text{c},h} \le P_{\text{av},h} \forall\, h \in \mathcal{H} && (15f)\\
& Q_{\text{c},h}^2 \le \Big(S_h^2 - \big(P_{\text{av},h} - P_{\text{c},h}\big)^2\Big) \forall\, h \in \mathcal{H} && (15g)\\
& |Q_{\text{c},h}| \le \tan\overline{\theta}\big(P_{\text{av},h} - P_{\text{c},h}\big) \forall\, h \in \mathcal{H}. && (15h)
\end{aligned}$$

Above, (15b)–(15c) capture voltages across the network; (15d)–(15e) force the voltage magnitudes to stay within defined limits $V_{\min}$ and $V_{\max}$; and (15f)–(15h) defines the set of feasible operating points of each inverter, with $\cos\overline{\theta}$ denoting the minimum allowable power factor.

Note that the problem above is a QCQP in the optimization variables $V, P_{\text{c}}, Q_{\text{c}}$. Key to ensuring this is the linearized expression for the voltage magnitudes. As such, this problem can be solved with lower computational burden compared to semidefinite programming methods, that we previously utilized in [6]. Notice further that by utilizing relations (7)–(8), the cost function and constraints in (15) can be expressed in terms of the powers $P_{\text{c}}, Q_{\text{c}}$, and the vector-valued variable V can be discarded. Next, we consider a further simplification/approximation that renders the problem to be a Linearly Constrained Quadratic Problem (LCQP).

C. SOID Problem: Special Case

If we consider a resistive network, where we neglect all reactive-power flows and injections, then the problem in (15) reduces to the following:

$$\begin{aligned}
\min_{P_{\text{c}}} \quad & C_{\text{opt}}(P_{\text{c}}) && (16a)\\
\text{subject to} \quad & V_{\min} \le 1 + \sum_{\ell \in \mathcal{N}'} R_{n\ell}\big(P_{\text{av},\ell} - P_{\text{c},\ell} - P_{\text{d},\ell}\big) \forall\, n \in \mathcal{N}' && (16b)\\
& V_{\max} \ge 1 + \sum_{\ell \in \mathcal{N}'} R_{n\ell}\big(P_{\text{av},\ell} - P_{\text{c},\ell} - P_{\text{d},\ell}\big) \forall\, n \in \mathcal{N}' && (16c)\\
& 0 \le P_{\text{c},h} \le P_{\text{av},h}, \forall\, h \in \mathcal{H}. && (16d)
\end{aligned}$$

The absence of (15g)–(15h) in this formulation, renders this problem formulation a LCQP. Although the problems described here and in the previous section are computationally affordable, distributed implementations leveraging the alternate direction method of multipliers are presented next to facilitate scalability to large distribution networks with limited information exchanges.

D. Distributed Implementation Leveraging ADMM

The main motivation for the development of a distributed solver for (15) is to enable utility and customers to pursue specific optimization objectives, while ensuring that system-level power-flow and voltage-regulation constraints are satisfied. To this end, ADMM is leveraged next to decouple utility- and customer-orientated objectives and constraints. Utility optimization includes minimizing power losses in the network and correcting voltage deviations. Customer based optimization includes minimizing the cost incurred in active power curtailment.

To this end, key is to introduce auxiliary vector-valued variables $\widetilde{P}$ and $\widetilde{Q}$ that represent copies of the inverter setpoints P and Q on the utility side. Using these new variables in the cost function in (14), the optimization problem (15) can be reformulated in the following equivalent way:

$$\begin{aligned}
\min_{\substack{V, \{P_{\text{c},h}, Q_{\text{c},h}\} \\ \{\widetilde{P}_h, \widetilde{Q}_h\}}} \quad & C_{\text{u}}\big(V, \widetilde{P}, \widetilde{Q}\big) + \sum_{\ell \in \mathcal{H}} C_{\text{c},\ell}\big(P_{\text{c},\ell}, Q_{\text{c},\ell}\big) \\
\text{subject to} \quad & \text{(15f)–(15h) and} \\
& \text{Re}\{V_n\} = 1 + \sum_{\ell \in \mathcal{N}'} \big(R_{n\ell}\widetilde{P}_\ell + X_{n\ell}\widetilde{Q}_\ell\big), \forall\, n \in \mathcal{N}' && (17a)\\
& \text{Im}\{V_n\} = \sum_{\ell \in \mathcal{N}'} \big(X_{n\ell}\widetilde{P}_\ell - R_{n\ell}\widetilde{Q}_\ell\big), \forall\, n \in \mathcal{N}' && (17b)\\
& V_{\min} \le 1 + \sum_{\ell \in \mathcal{N}'} R_{n\ell}\widetilde{P}_\ell + X_{n\ell}\widetilde{Q}_\ell, \forall\, n \in \mathcal{N}' \\
& V_{\max} \ge 1 + \sum_{\ell \in \mathcal{N}'} R_{n\ell}\widetilde{P}_\ell + X_{n\ell}\widetilde{Q}_\ell, \forall\, n \in \mathcal{N}' && (17c)\\
& \widetilde{P}_h = P_{\text{av},h} - P_{\text{c},h} - P_{\text{d},h}, \forall\, h \in \mathcal{H} && (17d)\\
& \widetilde{Q}_h = Q_{\text{c},h} - Q_{\text{d},h}, \forall\, h \in \mathcal{H}. && (17e)
\end{aligned}$$

The next steps involve the introduction of auxiliary variables to facilitate the decomposability of the constraints (17d) and (17e) across utility and inverters, and the partition of the linearized voltage expressions (17a) and (17b) into two groups: nodes with and without PV systems. Utility-related optimization variables, V, $\widetilde{P}$, and $\widetilde{Q}$, are collected in the set $\mathcal{O} := \{V, \widetilde{P}, \widetilde{Q}\}$. Customer-related decision variables, $P_{\rm c}$, $Q_{\rm c}$, are collected in the set $\mathcal{P}_h := \{P_{{\rm c},h}, Q_{{\rm c},h}, \forall h \in \mathcal{H}\}$ and $\mathcal{P}_{xy} := \{x_h, y_h, \forall h \in \mathcal{H}\}$ denotes the set that collects the auxiliary variables. Dual variables are collected in the set $\mathcal{D} := \{\underline{\lambda}_h, \lambda_h, \overline{\mu}_h, \mu_h, \forall h \in \mathcal{H}\}$; and $\kappa > 0$ is a given constant. Finally, $\mathcal{L}_u(\mathcal{O})$ and $\mathcal{L}_h(\mathcal{P}_h)$ denote the partial Lagrangian functions for the utility and customer side respectively, and they are spelled out in (24) and (25), respectively. Then, following the procedure provided in the Appendix and leveraging ADMM [22, Sec. 3.4], it can be shown that the distributed algorithm boils down to the steps **[S1]**-**[S2]** performed iteratively as described below (m represents the iteration index):

[S1a] Variables $V[m+1], \widetilde{P}_h[m+1], \widetilde{Q}_h[m+1]$ are updated as:

$$\begin{aligned}\mathcal{O} := \arg \min_{V, \{\widetilde{P}, \widetilde{Q}\}} \quad & \mathcal{L}_u\big(V, \widetilde{P}, \widetilde{Q}\big) \\ \text{subject to} \quad & \text{(22b)–(22c)} \quad \text{and} \\ & V_{\min} \le 1 + \sum_{\ell \in \mathcal{N}'} R_{n\ell} \widetilde{P}_\ell + \sum_{\ell \in \mathcal{N}'} X_{n\ell} \widetilde{Q}_\ell \\ & V_{\max} \ge 1 + \sum_{\ell \in \mathcal{N}'} R_{n\ell} \widetilde{P}_\ell \\ & \qquad + \sum_{\ell \in \mathcal{N}'} X_{n\ell} \widetilde{Q}_\ell, \forall\, n \in \mathcal{N}' \end{aligned} \tag{18}$$

[S1b] Variables $P_{{\rm c},h}[m+1], Q_{{\rm c},h}[m+1]$ are updated as:

$$\begin{aligned}\mathcal{P}_h := \arg \min_{\{P_{\rm c}, Q_{\rm c}\}} \quad & \mathcal{L}_h(P_{\rm c}, Q_{\rm c}) \\ \text{subject to} \quad & 0 \le P_{{\rm c},h} \le P_{{\rm av},h} \\ & Q_{{\rm c},h}^2 \le \Big(S_h^2 - \big(P_{{\rm av},h} - P_{{\rm c},h}\big)^2\Big) \\ & |Q_{{\rm c},h}| \le \tan\overline{\theta}\big(P_{{\rm av},h} - P_{{\rm c},h}\big)\ , \forall h \in \mathcal{H} \end{aligned} \tag{19}$$

[S2] Dual variables are updated as follows:

$$\begin{aligned}\lambda_h[m+1] = \lambda_h[m] + \frac{\kappa}{2}\big(&\widetilde{P}_h[m+1] - P_{{\rm av},h} + P_{{\rm d},h} \\ &+ P_{{\rm c},h}[m+1]\big) \end{aligned} \tag{20a}$$

$$\mu_h[m+1] = \mu_h[m] + \frac{\kappa}{2}\big(\widetilde{Q}_h[m+1] + Q_{{\rm d},h} - Q_{{\rm c},h}[m+1]\big). \tag{20b}$$

To implement the above algorithm, we require two-way communication of pertinent variables between utility and customers. For every iteration $m > 0$, (18) is solved on the utility side to update the variables in the set $\mathcal{O}$. Eventually PV-inverter setpoints satisfying power-quality objectives are obtained. Simultaneously, customer-side PV-inverter setpoints are updated via (19) and subsequently sent to the utility. Once these set points are exchanged, dual variables are updated at utility and customers through (20). While the problem setup considered here is different from that in [27], convergence of the algorithm described above to the solution of (15) can be shown leveraging [27, Proposition 1]. Finally, once the distributed algorithm is converged, all the PV-inverter set points are implemented at the PV inverters.

Algorithm 1 Distributed Scheme

Set $\lambda_h[0] = \mu_h[0] = 0$ for all $h \in \mathcal{H}$.
for $m = 1, 2, \ldots$ (repeat until convergence) **do**
1. **[Utility]**: update $\mathcal{O}[m+1]$ via (18).
   [Customer-h]: update $\mathcal{P}_h[m+1]$ via (19).
2. **[Utility]**: send $\mathcal{O}[m+1]\backslash|V|[m+1]$ to Customer; repeat for all $h \in \mathcal{H}$.
   [Customer-h]: receive $\mathcal{O}[m+1]\backslash|V|[m+1]$ from utility; send $\mathcal{P}_h[m+1]$ to utility; repeat for all $h \in \mathcal{H}$.
   [Utility]: receive $\mathcal{P}_h[m+1]$ from Customer; repeat for all $h \in \mathcal{H}$.
3. **[Utility]**: update $\{\lambda_h[m+1], \mu_h[m+1]\}_{h \in \mathcal{H}}$ via (20).
   [Customer-h]: update $\lambda_h[m+1], \mu_h[m+1]$ via (20); repeat for all $h \in \mathcal{H}$.

end for
Implement real and reactive setpoints in the PV inverters.

IV. Numerical Case Studies

We consider suitably modified versions of the IEEE 2500- and IEEE 123-node test feeders for the case studies. In particular, the IEEE 2500- and IEEE 123-node systems are used to illustrate improvements in the voltage profile across nodes using various renditions of the SOID strategies; while simulation results for the IEEE 123-node system help us to compare the accuracy with respect to SDP-based optimization methods in [6]. For all simulations, it is assumed that the network admittance matrix Y, available power $P_{\rm av}$, load demand $P_{\rm d}$, $Q_{\rm d}$ and inverter ratings S are known. Voltage limits $V_{\min}$ and $V_{\max}$ are set to 0.917 and 1.042 p.u., respectively [1]. The optimization package CVX [28] as part of MATLAB is used to run SOID and the distributed problem formulations proposed in this paper. Dc-ac derating coefficient for the PV systems is set to 0.77 [29]. Three different kind of dc ratings (5.52kW, 5.7kW and 9kW) have been used [30], [31]; and the PV inverters are oversized by 10% of the resultant ac rating [4]. The minimum power factor for the inverters is set to 0.85 [32]. System Advisory Model provided by NREL is used to compute active powers available during the day. Open Energy Info Database was used to obtain the load profile. For the simulations, the base load experienced in Saint Paul, MN, USA, during the month of July is utilized. All the plots are in accordance with the data considered during day time at 14:00. Finally, the voltage at the secondary of the step-down transformer (considered as the slack/reference bus in the model) is set to 1.02 p.u.

A. Accuracy of Linear Approximation

To demonstrate the accuracy of the linear approximation compared to the original nonlinear power-flow equations, we plot in Fig. 2 voltage magnitudes and phase angles recovered from the linear power-flow approximation and those obtained from the solution of the nonlinear power-flow equations (following [6]) for the IEEE 123-node test feeder system depicted

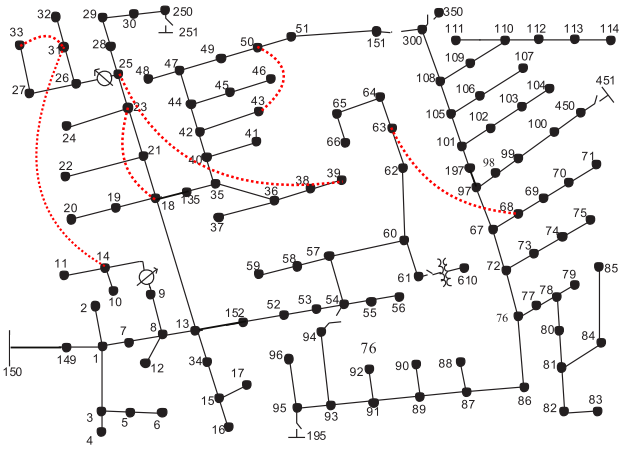

Fig. 1. IEEE 123-node distribution feeder with PV systems assumed to be present at nodes: 2, 4, 6, 10, 11, 12, 16, 17, 19, 20, 22, 24, 27, 32, 33, 36, 37, 38, 39, 41, 43, 46, 48, 49, 50, 51, 56, 59, 65, 66, 71, 75, 79, 83, 85, 88, 90, 92, 94, 96, 104, 107, 111, 114, 151, 250, 300, 450. Lines in dashed red indicate the modified meshed network that is also utilized in the case studies.

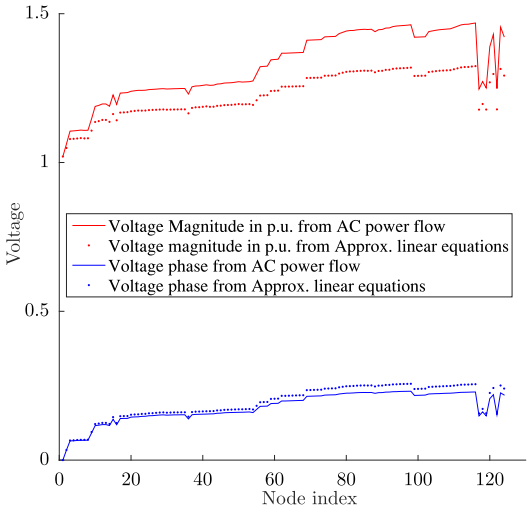

Fig. 2. Accuracy of linear approximation developed in Section II-C. Voltage magnitudes and phases for the nodes in the IEEE 123-node system are plotted from the linearized model and the original nonlinear power-flow equations.

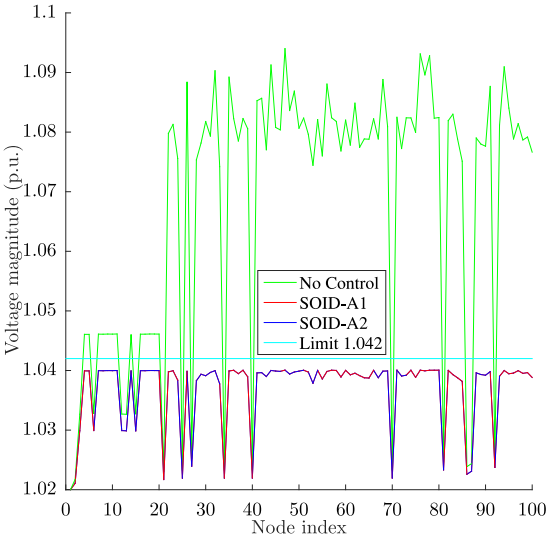

Fig. 3. Voltage profile across nodes in the network for SOID formulated in Section III-B for IEEE 2500-node system with radial structure.

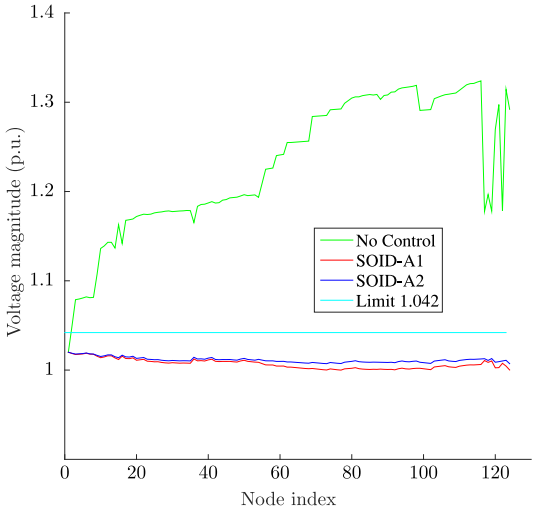

Fig. 4. Voltage profile across nodes in the network for SOID formulated in Section III-B for IEEE 123-node system with radial structure.

in Fig. 1. By and large, we see that errors are minimal; congruently problems formulated in Section III-B using this linear approximation offer computational speedup of up to 75%, which we further comment on in the next section. In Fig. 2, nodes with higher numbering are, in general, electrically more distant from the reference bus. Consequently, we see that errors increase as we move electrically further away from the reference bus. Nonetheless, it is worth mentioning that the errors conform to the bounds in [13] and [14].

B. SOID Plots for Different Cases

Results for the IEEE 2500-node test feeder system are plotted in Fig. 3 and for the IEEE 123-node test-feeder system in Fig. 4 and Fig. 5. Results for the modified IEEE 123-node meshed network are plotted in Fig. 6. The IEEE 123-node meshed network is obtained from suitably modifying the test feeder system by introducing lines as indicated by red dotted lines in Fig. 1. It should be noted that these voltage plots correspond to the nonlinear AC simulation of the original power flow equations. It can be seen that if no control strategy is implemented, then the upper voltage limit (plotted as a flat cyan line) is violated due to increased loading of the system. We implement two different cases, SOID-A1 and SOID-A2, with respect to the cost function in (14). Optimization parameters for strategy SOID-A1 are $c_\rho = 1$, $c_\phi = 1$, $c_v = 0$, $a_h = 0.1, b_h = c_h = d_h = 0$ (and results are plotted in red); for strategy SOID-A2, we penalize voltage deviations from the average by setting $c_\rho = 1$, $c_\phi = 1$, $c_v = 1$, $a_h = 0.1, b_h = c_h = d_h = 0$ (and results are plotted in dark blue). In Fig. 3, given space limits, we plot only the voltages for the first 100 nodes to demonstrate that the system is operating at prescribed limits. The average computational time required to solve the problem formulated in Section III-B for IEEE 2500-node system was 600 sec; the computation times for the different cases corresponding to the

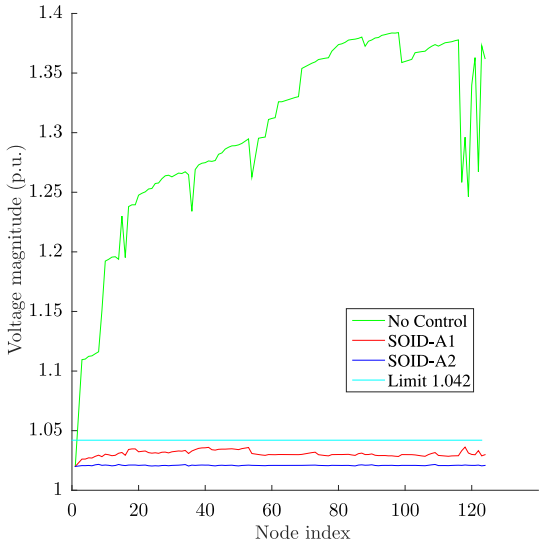

Fig. 5. Voltage profile across nodes in the network for SOID formulated in Section III-C for IEEE 123-node system with radial structure.

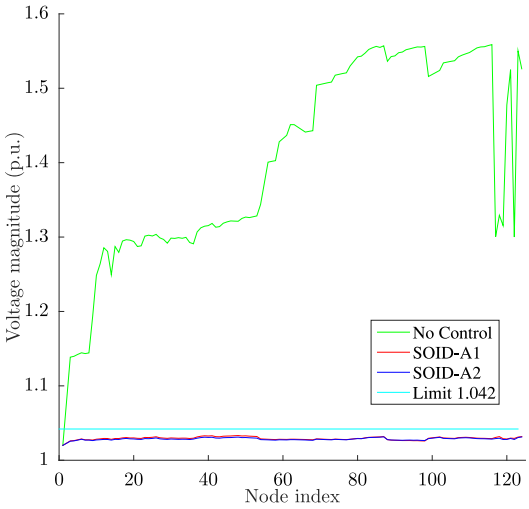

Fig. 6. Voltage profile across nodes in the network for SOID formulated in Section III-B for IEEE 123-node system with mesh structure.

IEEE 123-node system are tabulated in Table I. (Note that the computational time is calculated with reference to time when no control strategy is implemented and hence, the first row of the table contains 0's.) The computation times for the meshed network are not reported, since they are approximately the same as those in Table I. This table also provides a comparison with the OID framework setup proposed in [6]. The simulation was run on a machine with an Intel core i7-4710HQ CPU @ 2.5 GHz. It can be seen that as we progress by adding objective terms one at a time to the cost function from 'No Control Strategy' to 'SOID-A2', the average computational time increases.

C. Convergence of the Distributed Algorithm

Parameters to analyze convergence of the distributed scheme are set as follows: $a_h = 0.1$ and $b_h = 0$. The ADMM constant

TABLE I
AVERAGE COMPUTATIONAL TIME IN (sec) FOR IEEE 123-NODE TEST FEEDER SYSTEM

Cases in Fig. 4	SOID in Section III-B	SDP-OID
No Control	0	0
SOID - A1	2.01	34.7
SOID - A2	2.51	54.07

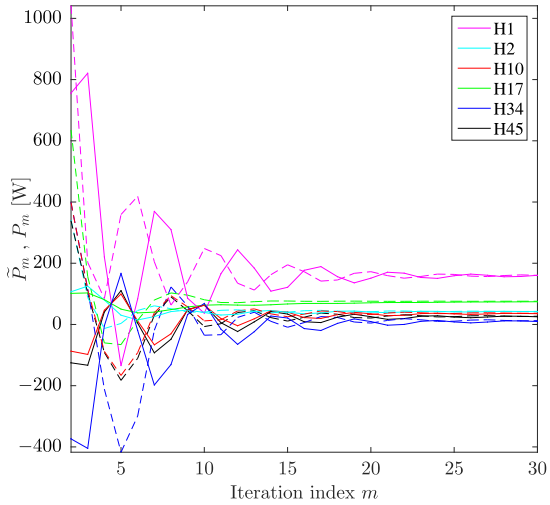

Fig. 7. Convergence of the distributed algorithm.

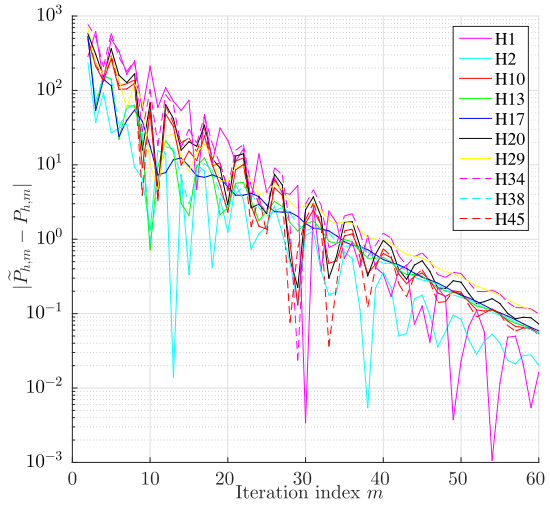

Fig. 8. Error plot for power curtailment.

κ is set equal to 5. Solar irradiance conditions at 14:00 are utilized for this particular case. Figure 7 depicts the trajectories of the iterates $\{\widetilde{P}_h[m]\}_{h\in\mathcal{H}}$ (solid lines) and $\{P_h[m]\}_{h\in\mathcal{H}}$ (dashed lines) for a certain set of selected houses among $H_1 - H_{48}$. Finally, the trajectories of error tracking differences between $|\widetilde{P}_h[m] - P_h[m]|$, as a function of the ADMM iteration index are depicted in Fig. 8. It can be clearly seen that the algorithm converges to a set-point that is optimal to both the utility and customers.

V. CONCLUSION

This paper developed a suite of scalable algorithms to determine the active- and reactive-power set points for

photovoltaic (PV) inverters in residential distribution networks. A linear expression for the voltages expressed in rectangular coordinates was leveraged to get around the non-convexity that would otherwise be encountered in the AC-OPF setting. First, we formulated a quadratic constrained quadratic program (QCQP) by leveraging a linear approximation of the algebraic power-flow equations that ensures optimization of inverter dispatch (quantified, e.g., through power losses, correcting voltage deviations). This was then reduced to a LCQP for resistive dominant networks. A distributed scheme was also proposed to promote scalability and further reduce the computational burden of the optimization problem. Added advantage of the distributed algorithm is that it outlines avenues for the formulation and operation of distribution-network markets. The merits of the proposed approach were demonstrated using a comprehensive set of simulation results that utilized real-world PV-generation and load-profile data for illustrative low-voltage residential distribution system test cases.

As part of future work, the proposed SOID problems and the distributed versions will be implemented in hardware setups using micro-controllers and a suitable communication medium. We will also study communication-related issues, as well as further simplifications of the optimization problem to make it suitable for practical implementation. An example of such a simplification would be to express the operating region of the PV inverters entirely with linear constraints. Additionally, we will also focus on adopting the approaches suggested in this work for unbalanced multi-phase networks. Also, we will compare the results for the problems (and distributed implementations) with approaches such as SOCP and belief propagation.

APPENDIX

A. Expression for Power Losses in (11)

Begin by expressing the voltage at the m node in the network as $V_m = \mathrm{Re}\{V_m\} + \mathrm{j}\,\mathrm{Im}\{V_m\}$. The expression in (11) can be derived as follows:

$$\begin{aligned}\rho(V,I) &= \sum_{(m,n)\in\mathcal{E}} \mathrm{Re}\Big\{V_m I^*_{(m,n)}\Big\} - \mathrm{Re}\Big\{V_n I^*_{(m,n)}\Big\}\\ &= \sum_{(m,n)\in\mathcal{E}} \mathrm{Re}\big\{V_m\big(V^*_m - V^*_n\big)y^*_{mn}\big\}\\ &\quad - \mathrm{Re}\big\{V_n\big(V^*_m - V^*_n\big)y^*_{mn}\big\}\\ &= \sum_{(m,n)\in\mathcal{E}} \mathrm{Re}\big\{\big(V_m\big(V^*_m - V^*_n\big) - V_n\big(V^*_m - V^*_n\big)\big)y^*_{mn}\big\}.\end{aligned}$$

Expanding the expression above with the rectangular-form adopted for the nodal voltages, we get:

$$\begin{aligned}\rho(V,I) = \sum_{(m,n)\in\mathcal{E}} \mathrm{Re}\big\{y^*_{mn}\big\}\Big(&(\mathrm{Re}\{V_m\} + \mathrm{Re}\{V_n\})^2\\ &+ (\mathrm{Im}\{V_m\} + \mathrm{Im}\{V_n\})^2\Big).\end{aligned} \tag{21}$$

Other loss modeling methods have been proposed in the literature and could potentially be applied in this setting; one example is [11].

B. Derivation of the ADMM-Based Distributed Algorithm

Beginning with (17), the standard procedure is to dualize constraints (17d) and (17e), and subsequently leverage the decomposability of the associated Lagrangian function. However, to favor decomposability of quadratically augmented Lagrangian functions [22, Sec. 3.4], consider first introducing auxiliary variables x_h, y_h and reformulating (17) in the following equivalent way:

$$\min_{\substack{V,\{P_{\mathrm{c},h},Q_{\mathrm{c},h}\}\\ \{\widetilde{P},\widetilde{Q},x_h,y_h\}}} \quad C_{\mathrm{u}}\big(V,\widetilde{P},\widetilde{Q}\big) + \sum_{\ell\in\mathcal{H}} C_{\mathrm{c},\ell}\big(P_{\mathrm{c},\ell},Q_{\mathrm{c},\ell}\big) \tag{22a}$$

$$\text{subject to} \quad \text{(15f)–(15h) and}$$

$$\mathrm{Re}\{V_n\} = 1 + \sum_{\ell\in\mathcal{H}}\big(R_{n\ell}\widetilde{P}_\ell + X_{n\ell}\widetilde{Q}_\ell\big) - \sum_{\ell\in\mathcal{N}'\setminus\mathcal{H}}\big(R_{n\ell}P_{\mathrm{d},\ell} + X_{n\ell}Q_{\mathrm{d},\ell}\big)\ \forall\, n\in\mathcal{N}' \tag{22b}$$

$$\mathrm{Im}\{V_n\} = \sum_{\ell\in\mathcal{H}}\big(X_{n\ell}\widetilde{P}_\ell - R_{n\ell}\widetilde{Q}_\ell\big) - \sum_{\ell\in\mathcal{N}'\setminus\mathcal{H}}\big(X_{n\ell}P_{\mathrm{d},\ell} - R_{n\ell}Q_{\mathrm{d},\ell}\big)\ \forall\, n\in\mathcal{N}' \tag{22c}$$

$$V_{\min} \le 1 + \sum_{\ell\in\mathcal{N}'} R_{n\ell}\widetilde{P}_\ell + \sum_{\ell\in\mathcal{N}'} X_{n\ell}\widetilde{Q}_\ell$$

$$V_{\max} \ge 1 + \sum_{\ell\in\mathcal{N}'} R_{n\ell}\widetilde{P}_\ell + \sum_{\ell\in\mathcal{N}'} X_{n\ell}\widetilde{Q}_\ell,\ \forall\, n\in\mathcal{N}'$$

$$\widetilde{P}_h = x_h\ \forall\, h\in\mathcal{H} \tag{22d}$$

$$x_h = P_{\mathrm{av},h} - P_{\mathrm{d},h} - P_{\mathrm{c},h}\ \forall\, h\in\mathcal{H} \tag{22e}$$

$$\widetilde{Q}_h = y_h\ \forall\, h\in\mathcal{H} \tag{22f}$$

$$y_h = -Q_{\mathrm{d},h} + Q_{\mathrm{c},h},\ \forall\, h\in\mathcal{H}. \tag{22g}$$

Now, (22) can be solved in a distributed fashion by dualizing constraints (22d)–(22g) and leveraging ADMM [22, Sec. 3.4]. To this end, let $\lambda_h, \overline{\lambda}_h, \mu_h, \overline{\mu}_h$ be the Lagrange multipliers associated with (22d)–(22g), where h is the inverter index. Then the quadratically augmented Lagrangian can be obtained as:

$$\begin{aligned}&\mathcal{L}\big(\mathcal{O},\mathcal{P}_h,\mathcal{P}_{xy},\mathcal{D}\big)\\ &\quad\coloneqq C_{\mathrm{u}}\big(V,\widetilde{P},\widetilde{Q}\big) + \sum_{\ell\in\mathcal{H}} C_{\mathrm{c},\ell}\big(P_{\mathrm{c},\ell},Q_{\mathrm{c},\ell}\big)\\ &\qquad + \sum_{h\in\mathcal{H}}\big(\lambda_h\big(\widetilde{P}_h - x_h\big) + \overline{\lambda}_h\big(x_h - P_{\mathrm{av},h} + P_{\mathrm{d},h} + P_{\mathrm{c},h}\big)\big)\\ &\qquad + \sum_{h\in\mathcal{H}}\big(\mu_h\big(\widetilde{Q}_h - y_h\big) + \overline{\mu}_h\big(y_h + Q_{\mathrm{d},h} - Q_{\mathrm{c},h}\big)\big)\\ &\qquad + \sum_{h\in\mathcal{H}}\Big(\frac{\kappa}{2}\big(\widetilde{P}_h - x_h\big)^2 + \frac{\kappa}{2}\big(x_h - P_{\mathrm{av},h} + P_{\mathrm{d},h} + P_{\mathrm{c},h}\big)^2\Big)\\ &\qquad + \sum_{h\in\mathcal{H}}\Big(\frac{\kappa}{2}\big(\widetilde{Q}_h - y_h\big)^2 + \frac{\kappa}{2}\big(y_h + Q_{\mathrm{d},h} - Q_{\mathrm{c},h}\big)^2\Big)\end{aligned} \tag{23}$$

where utility related optimization variables are collected in $\mathcal{O} \coloneqq \{V,\widetilde{P},\widetilde{Q}\}$; Customer related decision variables are collected in $\mathcal{P}_h \coloneqq \{P_{\mathrm{c},h}, Q_{\mathrm{c},h}, \forall h\in\mathcal{H}\}$; $\mathcal{P}_{xy} \coloneqq \{x_h, y_h, \forall h\in\mathcal{H}\}$ is the set of auxiliary variables; Dual variables are collected in $\mathcal{D} \coloneqq \{\overline{\lambda}_h, \lambda_h, \overline{\mu}_h, \mu_h, \forall h\in\mathcal{H}\}$; and $\kappa > 0$ is a given constant. Using [27, Lemma 1] and (23) we can define individual partial

Lagrangian functions for utility as $\mathcal{L}_u(\mathcal{O})$ and customer side as $\mathcal{L}_h(\mathcal{P}_h)$ for the mth iteration as below:

$$\begin{aligned}\mathcal{L}_u(\mathcal{O}) \coloneqq\ & C_{\mathrm{u}}\big(V, \widetilde{P}, \widetilde{Q}\big) + \sum_{h\in\mathcal{H}} \frac{\kappa}{2}\Big(\widetilde{P}^2 + \widetilde{Q}^2\Big) \\ & + \sum_{h\in\mathcal{H}} \widetilde{P}_h\Big(\lambda_h[m] - \frac{\kappa}{2}\big(\widetilde{P}_h[m] + P_{\mathrm{av},h} \\ & \qquad - P_{\mathrm{d},h} - P_{\mathrm{c},h}[m]\big)\Big) \\ & + \sum_{h\in\mathcal{H}} \widetilde{Q}_h\Big(\mu_h[m] - \frac{\kappa}{2}\big(\widetilde{Q}_h[m] - Q_{\mathrm{d},h} + Q_{\mathrm{c},h}[m]\big)\Big)\end{aligned} \tag{24}$$

$$\begin{aligned}\mathcal{L}_h(\mathcal{P}_h) \coloneqq\ & C_{c,h}\big(P_{\mathrm{c},h}, Q_{\mathrm{c},h}\big) + \sum_{h\in\mathcal{H}} \frac{\kappa}{2}\Big(P_{\mathrm{c},h}^2 + Q_{\mathrm{c},h}^2\Big) \\ & + P_{\mathrm{c},h}\Big(\lambda_h[m] - \frac{\kappa}{2}\big(-P_{\mathrm{c},h}[m] - P_{\mathrm{av},h} \\ & \qquad + P_{\mathrm{d},h} - \widetilde{P}_h[m]\big)\Big) \\ & + Q_{\mathrm{c},h}\Big(-\mu_h[m] - \frac{\kappa}{2}\big(\widetilde{Q}_h[m] + Q_{\mathrm{d},h} + Q_{\mathrm{c},h}[m]\big)\Big).\end{aligned} \tag{25}$$

By minimizing the respective partial Lagrangian function at the utility and inverter sides, one obtains steps [S1]–[S2]. It is also worth mentioning that various techniques have been proposed in the literature to select the value of κ with a view towards improving convergence, see, e.g., [33] and [34].

REFERENCES

[1] R. Tonkoski, L. A. C. Lopes, and T. H. El-Fouly, "Coordinated active power curtailment of grid connected PV inverters for overvoltage prevention," *IEEE Trans. Sustain. Energy*, vol. 2, no. 2, pp. 139–147, Apr. 2011.

[2] A. Samadi, R. Eriksson, L. Söder, B. G. Rawn, and J. C. Boemer, "Coordinated active power-dependent voltage regulation in distribution grids with PV systems," *IEEE Trans. Power Del.*, vol. 29, no. 3, pp. 1454–1464, Jun. 2014.

[3] P. Jahangiri and D. C. Aliprantis, "Distributed volt/var control by PV inverters," *IEEE Trans. Power Syst.*, vol. 28, no. 3, pp. 3429–3439, Aug. 2013.

[4] K. Turitsyn, P. Sulc, S. Backhaus, and M. Chertkov, "Options for control of reactive power by distributed photovoltaic generators," *Proc. IEEE*, vol. 99, no. 6, pp. 1063–1073, Jun. 2011.

[5] A. Cagnano, E. De Tuglie, M. Liserre, and R. A. Mastromauro, "Online optimal reactive power control strategy of PV inverters," *IEEE Trans. Ind. Electron.*, vol. 58, no. 10, pp. 4549–4558, Oct. 2011.

[6] E. Dall'Anese, S. V. Dhople, and G. B. Giannakis, "Optimal dispatch of photovoltaic inverters in residential distribution systems," *IEEE Trans. Sustain. Energy*, vol. 5, no. 2, pp. 487–497, Apr. 2014.

[7] J. Lavaei and S. H. Low, "Zero duality gap in optimal power flow problem," *IEEE Trans. Power Syst.*, vol. 27, no. 1, pp. 92–107, Feb. 2012.

[8] Y. Nesterov, A. Nemirovskii, and Y. Ye, *Interior-Point Polynomial Algorithms in Convex Programming*, vol. 13. Philadelphia, PA, USA: SIAM, 1994.

[9] E. De Klerk, "Exploiting special structure in semidefinite programming: A survey of theory and applications," *Eur. J. Oper. Res.*, vol. 201, no. 1, pp. 1–10, 2010.

[10] R. Madani, M. Ashraphijuo, and J. Lavaei, "Promises of conic relaxation for contingency-constrained optimal power flow problem," *IEEE Trans. Power Syst.*, vol. 31, no. 2, pp. 1297–1307, Mar. 2016.

[11] R. A. Jabr, "Radial distribution load flow using conic programming," *IEEE Trans. Power Syst.*, vol. 21, no. 3, pp. 1458–1459, Aug. 2006.

[12] C. Coffrin, H. L. Hijazi, and P. Van Hentenryck, "The QC relaxation: A theoretical and computational study on optimal power flow," *IEEE Trans. Power Syst.*, to be published.

[13] S. Bolognani and S. Zampieri, "On the existence and linear approximation of the power flow solution in power distribution networks," *IEEE Trans. Power Syst.*, vol. 31, no. 1, pp. 163–172, Jan. 2016.

[14] S. V. Dhople, S. S. Guggilam, and Y. C. Chen. (2015). *Linear Approximations to AC Power Flow in Rectangular Coordinates*. [Online]. Available: http://arxiv.org/abs/1512.06903

[15] J. de Hoog, T. Alpcan, M. Brazil, D. A. Thomas, and I. Mareels, "Optimal charging of electric vehicles taking distribution network constraints into account," *IEEE Trans. Power Syst.*, vol. 30, no. 1, pp. 365–375, Jan. 2015.

[16] A. J. Wood and B. F. Wollenberg, *Power Generation, Operation, and Control*. Hoboken, NJ, USA: Wiley, 2012.

[17] L. Gan and S. H. Low, "Convex relaxations and linear approximation for optimal power flow in multiphase radial networks," in *Proc. Power Syst. Comput. Conf. (PSCC)*, Wrocław, Poland, 2014, pp. 1–9.

[18] R. P. O'Neill, A. Castillo, and M. B. Cain. (2012). *The IV Formulation and Linear Approximations of the AC Optimal Power Flow Problem*. [Online]. Available: https://www.ferc.gov/industries/electric/indus-act/market-planning/opf-papers/acopf-2-iv-linearization.pdf

[19] H. Zhang, V. Vittal, G. T. Heydt, and J. Quintero, "A relaxed AC optimal power flow model based on a Taylor series," in *Proc. IEEE Innov. Smart Grid Technol. Asia (ISGT Asia)*, Bengaluru, India, 2013, pp. 1–5.

[20] A. M. C. A. Koster and S. Lemkens, "Designing AC power grids using integer linear programming," in *Network Optimization*. Heidelberg, Germany: Springer-Verlag, 2011, pp. 478–483.

[21] E. Dall'Anese, S. V. Dhople, and G. B. Giannakis, "Photovoltaic inverter controllers seeking AC optimal power flow solutions," *IEEE Trans. Power Syst.*, to be published.

[22] D. P. Bertsekas and J. N. Tsitsiklis, *Parallel and Distributed Computation: Numerical Methods*. Englewood Cliffs, NJ, USA: Prentice-Hall, 1989.

[23] S. Boyd, N. Parikh, E. Chu, B. Peleato, and J. Eckstein, "Distributed optimization and statistical learning via the alternating direction method of multipliers," *Found. Trends Mach. Learn.*, vol. 3, no. 1, pp. 1–122, 2011.

[24] P. Scott and S. Thiebaux, "Distributed multi-period optimal power flow for demand response in microgrids," in *Proc. ACM 6th Int. Conf. Future Energy Syst.*, Bengaluru, India, 2015, pp. 17–26.

[25] P. Šulc, S. Backhaus, and M. Chertkov, "Optimal distributed control of reactive power via the alternating direction method of multipliers," *IEEE Trans. Energy Convers.*, vol. 29, no. 4, pp. 968–977, Dec. 2014.

[26] T. Erseghe, D. Zennaro, E. Dall'Anese, and L. Vangelista, "Fast consensus by the alternating direction multipliers method," *IEEE Trans. Signal Process.*, vol. 59, no. 11, pp. 5523–5537, Nov. 2011.

[27] E. Dall'Anese, S. V. Dhople, B. B. Johnson, and G. B. Giannakis, "Decentralized optimal dispatch of photovoltaic inverters in residential distribution systems," *IEEE Trans. Energy Convers.*, vol. 29, no. 4, pp. 957–967, Dec. 2014.

[28] M. Grant, S. Boyd, and Y. Ye. (2008). *CVX: MATLAB Software for Disciplined Convex Programming*. [Online]. Available: http://cvxr.com/cvx/

[29] D. L. King, S. Gonzalez, G. M. Galbraith, and W. E. Boyson, "Performance model for grid-connected photovoltaic inverters," Sandia Nat. Lab., Albuquerque, NM, USA, Tech. Rep. SAND 2007-5036, 2007.

[30] S. T. Cady, D. Mestas, and C. Cirone, "Engineering systems in the Re_home: A net-zero, solar-powered house for the U.S. Department of Energy's 2011 Solar Decathlon," in *Proc. IEEE Power Energy Conf. Illinois (PECI)*, Champaign, IL, USA, 2012, pp. 1–5.

[31] S. V. Dhople, J. L. Ehlmann, C. J. Murray, S. T. Cady, and P. L. Chapman, "Engineering systems in the gable home: A passive, net-zero, solar-powered house for the U.S. Department of Energy's 2009 Solar Decathlon," in *Proc. Power Energy Conf. Illinois (PECI)*, Urbana, IL, USA, 2010, pp. 58–62.

[32] T. Stetz, J. Künschner, M. Braun, and B. Engel, "Cost-optimal sizing of photovoltaic inverters—Influence of new grid codes and cost reductions," in *Proc. 25th Eur. PV Solar Energy Conf. Exhibit.*, Valencia, Spain, 2010, pp. 4633–4639.

[33] E. Ghadimi, A. Teixeira, I. Shames, and M. Johansson, "Optimal parameter selection for the alternating direction method of multipliers (ADMM): Quadratic problems," *IEEE Trans. Autom. Control*, vol. 60, no. 3, pp. 644–658, Mar. 2015.

[34] A. U. Raghunathan and S. Di Cairano, "Optimal step-size selection in alternating direction method of multipliers for convex quadratic programs and model predictive control," in *Proc. Symp. Math. Theory Netw. Syst.*, Groningen, The Netherlands, 2014, pp. 807–814.

Swaroop S. Guggilam (S'15) received the bachelor's degree from Veermata Jijabai Technological Institute, Mumbai, India, in 2013, and the M.S. degree from the University of Minnesota, Minneapolis, MN, USA, in 2015, where he is currently pursuing the Ph.D. degree, all in electrical engineering.

His research interests include distribution networks, optimization, power system modeling, and analysis and control for increasing renewable integration.

Emiliano Dall'Anese (S'08–M'11) received the Laurea Triennale (B.Sc.) degree and the Laurea Specialistica (M.Sc.) degree in telecommunications engineering from the University of Padova, Italy, in 2005 and 2007, respectively, and the Ph.D. degree in information engineering from the Department of Information Engineering, University of Padova, in 2011. From 2009 to 2010, he was a Visiting Scholar with the Department of Electrical and Computer Engineering, University of Minnesota, USA, where he was a Post-Doctoral Associate with the Department of Electrical and Computer Engineering and the Digital Technology Center from 2011 to 2014. Since 2014, he has been a Senior Engineer with the National Renewable Energy Laboratory, Golden, CO, USA.

His current research focuses on distributed optimization and control of power distribution networks with distributed energy resources and statistical inference for data analytics.

Yu Christine Chen (S'10–M'15) received the B.A.Sc. degree in engineering science from the University of Toronto, Toronto, ON, Canada, in 2009, and the M.S. and Ph.D. degrees in electrical engineering from the University of Illinois at Urbana–Champaign, Urbana, IL, USA, in 2011 and 2014, respectively.

She is currently an Assistant Professor with the Department of Electrical and Computer Engineering, University of British Columbia, Vancouver, BC, Canada, where she is affiliated with the Electric Power and Energy Systems Group. Her research interests include power system analysis, monitoring, and control.

Sairaj V. Dhople (S'09–M'13) received the B.S., M.S., and Ph.D. degrees in electrical engineering from the University of Illinois at Urbana–Champaign in 2007, 2009, and 2012, respectively. He is currently an Assistant Professor with the Department of Electrical and Computer Engineering, University of Minnesota, Minneapolis, where he is affiliated with the Power and Energy Systems Research Group. His research interests include modeling, analysis, and control of power electronics and power systems with a focus on renewable integration. He was a recipient of the NSF CAREER Award in 2015. He currently serves as an Associate Editor of the IEEE TRANSACTIONS ON ENERGY CONVERSION.

Georgios B. Giannakis (S'84–M'86–SM'91–F'97) received the diploma degree in electrical engineering from the National Technical University of Athens, Greece, in 1981; the M.Sc. degree in electrical engineering in 1983; the M.Sc. degree in mathematics in 1986; and the Ph.D. degree in electrical engineering in 1986 from the University of Southern California. Since 1999, he has been a Professor with the University of Minnesota, where he is currently an ADC Chair in Wireless Telecommunications with the Electrical and Computer Engineering Department. He serves as the Director of the Digital Technology Center.

His general interests span the areas of communications, networking, and statistical signal processing. He has published over 375 journal papers, 635 conference papers, 22 book chapters, two edited books, and two research monographs (H-index 113) in the above areas. He is the (Co-)Inventor of 25 patents issued. His current research focuses on learning from big data, wireless cognitive radios, and network science with applications to social, brain, and power networks with renewables. He was a recipient of the Technical Achievement Awards from the Signal Processing (SP) Society in 2000 and EURASIP in 2005, the Young Faculty Teaching Award, the G. W. Taylor Award for Distinguished Research from the University of Minnesota, the IEEE Fourier Technical Field Award in 2015, and was a co-recipient of eight best paper awards from the IEEE SP and Communications Societies, including the G. Marconi Prize Paper Award in Wireless Communications. He has served the IEEE in a number of posts, including the Distinguished Lecturer for the IEEE-SP Society. He is a fellow of EURASIP.